ELSEVIER

Polymer 41 (2000) 809–812

polymer

Polymer Communication

Magnetic orientation of poly(ethylene terephthalate)

T. Kimura*, T. Kawai, Y. Sakamoto

Department of Applied Chemistry, Tokyo Metropolitan University, 1-1 Minami-ohsawa, Hachioji, Tokyo 192-0397, Japan

Received 10 May 1999; accepted 24 May 1999

Abstract

A new finding is reported on the magnetic orientation of poly(ethylene terephthalate) (PET) in the magnetic field of 6 T. The orientation is observed to start during the induction period of isothermal crystallization from melt. This observation is in accord with the observation that we made for the magnetic orientation of other two crystalline polymers, i.e. poly(ethylene-2,6-naphthalate) and isotactic polystyrene, reported in our previous papers. The results obtained in this study is in support of the assumption that some ordered structure formed during the induction period is responsible for the magnetic orientation though the detail of this ordered structure is still open to discussion. Crystallites formed after a prolonged crystallization time exhibited the orientation with a^*-axis roughly aligned perpendicular to the magnetic field. This alignment of a^*-axis is explained in terms of the diamagnetic susceptibility of the aromatic ring in the crystal of PET.

Keywords: Magnetic orientation; Magnetic birefringence; Poly(ethylene terephthalate)

1. Introduction

Liquid crystalline polymers align under magnetic fields, while crystalline polymers in their molten state were considered to be unable to align in the magnetic field, except a low degree of alignment due to Cotton–Mouton effect, because the melts are isotropic and lack in anisotropic domains necessary for the magnetic orientation. There are very few studies reporting about anisotropic structures in melt in connection with the magnetic orientation [1]. However, we have recently reported that poly(ethylene-2,6-naphthalate) (PEN) and isotactic polystyrene (iPS), both are crystalline polymers, align under magnetic field during the induction period of the crystallization from melts [2–5]. In order to explain this phenomenon, we have assumed that some ordered structures are formed during the induction period of the melt crystallization and they align under the magnetic field in a fashion similar to the magnetic orientation of liquid crystalline polymers. Infrared spectroscopic studies have provided evidence supporting the existence of these ordered structures [6,7].

The ordered structures which we have assumed to occur for PEN and iPS do not seem peculiar to these polymers, but they might occur in other crystalline polymers in common. Some crystalline polymers exhibit stable liquid crystalline phases and hence are referred to as liquid crystalline polymers. On the contrary, majority of the crystalline polymers are not classified as liquid crystalline polymers because they do not form liquid crystalline phases in a clear and stable manner. However, mesophase [8–10], including liquid crystal and conformationally disordered crystal phases, could occur between the isotropic melt and the crystal though they may be unstable and transient. In this view, we could expect that crystalline polymers could undergo magnetic orientation in general if a magnetic field is applied to the mesophase which occurs during the crystallization process, most likely during the induction period.

Formation of liquid-crystalline-like structures in poly(ethylene terephthalate) (PET) has been reported [11] to occur during the induction period of cold crystallization. In addition, our preliminary results [12,13] on PET have provided evidence supporting the scheme of the magnetic orientation mentioned above. In this paper, we report on the magnetic orientation of PET observed during the melt crystallization. The condition of the magnetic orientation and the analyses of the aligned structures are presented.

2. Experimental

2.1. Sample preparation

Pellets of PET (M_w = ca. 10 000) supplied by Asahi Chemical were dried and pressed at 290°C for 5 min and

* Corresponding author. Tel.: +81-426-77-2845; fax: +81-426-77-2821.
E-mail address: kimura-tsunehisa@c.metro-u.ac.jp (T. Kimura)

0032-3861/00/$ - see front matter
PII: S0032-3861(99)00451-6

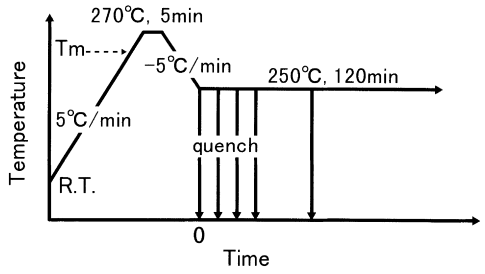

Fig. 1. Thermal history applied for the in situ birefringence measurements as well as for the preparation of samples quenched at different points of crystallization time. The origin of the crystallization time (time zero in the figure) is taken as the time at which the temperature becomes 250°C. Experiments were carried out inside as well as outside the magnet (6 T). For the experiments in the magnet, the magnetic field was applied from the beginning, before the heating from the room temperature until the completion of the experiment.

allowed to quench in ice water to obtain a pressed film. The pressed film thus obtained was dried under vacuum for 24 h. The thickness was ca. 50 and 200 μm. The preparation of the samples, of which the crystallization was interrupted by quenching at various periods of crystallization time, was carried out using 200 μm films in a furnace designed for the heat treatment in the magnet. The detail of the furnace is reported elsewhere [3]. The heat-treated samples thus obtained were subjected to further analyses including the X-ray and optical azimuthal analyses.

2.2. Wide angle X-ray measurements

Wide angle X-ray diffraction (WAXD) measurements were carried out by using a MAC Science MXP system operated at 40 kV and 250 mA to generate Ni-filtered CuKα X-ray beam.

2.3. Optical measurements

An Olympus BH-2 microscope equipped with a photo monitor was used for the measurements of the azimuthal angle dependence of the heat-treated samples. By rotating the sample under the crossed polar condition, the transmitting light intensity changes as $I^2 \sim \sin^2(2\phi)$, giving maxima at 45, 135, 225 and 315°, enabling the detection of the orientation. Here, ϕ is the azimuthal angle with respect to the orientation direction. In situ measurements for the change in transmitting light intensity under the crossed polars were carried out by using 50 μm films in a home-built apparatus whose detail is reported elsewhere [4]. The measurements were carried out both in a super conducting magnet (6 T) and outside the magnet. The direction of the magnetic field makes an angle of 45° with respect to the analyzer. Formation of the anisotropic structure whether they are aligned uniaxially or distributed randomly is detected by the change in the transmitting light intensity observed under the crossed polars. The intensity changes according to $I^2 \sim \sin^2(\pi d\Delta n/\lambda)$, where d, Δn, and λ are the sample thickness, the birefringence, and the wavelength of the light, respectively.

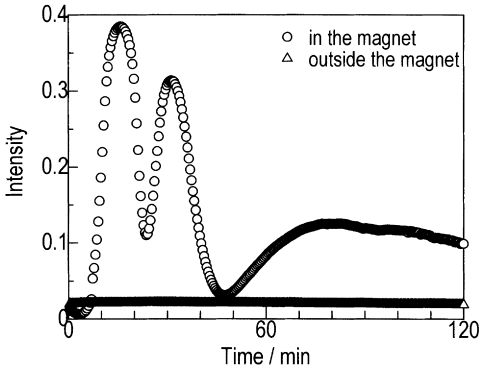

Fig. 2. Change in the transmitting light intensity measured under the crossed polars during the crystallization at 250°C after melting at 270°C. Sample thickness is 50 μm.

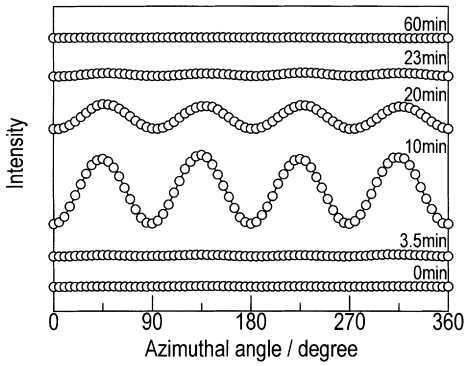

Fig. 3. Optical azimuthal scans for the samples melted at 270°C and crystallized at 250°C, followed by quenching at various periods of crystallization time indicated in the figure. Heat treatment was made in the magnet. Zero azimuthal angle corresponds to the direction of the magnetic field. Sample thickness is 200 μm.

2.4. Differential scanning calorimetry

DSC measurement was carried out using a SEIKO DSC200 equipped with a thermal analysis system SSC5200H under a dry nitrogen atmosphere. The pressed film was heated at a heating rate of 5°C/min. The melting point (T_m), defined as the top of the endothermic peak was 261°C. Measurements was performed without the magnetic field.

3. Results and discussion

In Fig. 1 is shown the diagram describing the thermal process used both for the birefringence measurements and for the preparation of the samples, for which the crystallization was interrupted by quenching at various periods of crystallization time. The pressed film sample was heated from the room temperature at 5°C/min, melted at 270°C for 5 min, cooled at 5°C/min down to 250°C and subjected to the isothermal crystallization.

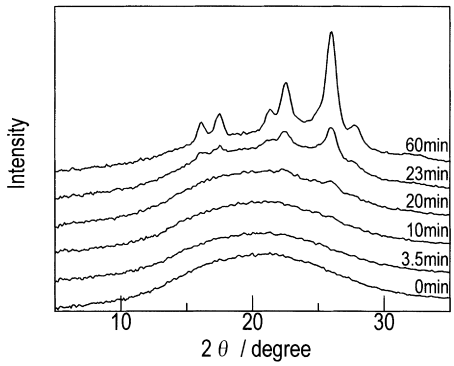

Fig. 4. Wide angle X-ray equatorial scans for the samples melted at 270°C and crystallized at 250°C, followed by quenching at various periods of crystallization time indicated in the figure. The equatorial direction corresponds to the direction perpendicular to the magnetic field. Sample thickness is 200 μm.

The results of the birefringence measurements are shown in Fig. 2. For the measurement in the magnet, a sinusoidal change of the transmitting light intensity is observed under the crossed polars. The sinusoidal change is due to the increase in Δn, as indicated by the equation $I^2 \sim \sin^2(\pi d\Delta n/\lambda)$, caused by a macroscopic orientation. On the contrary, the measurement outside the magnet shows little change in the transmitting light intensity, indicating that no orientation occurs.

In order to confirm the magnetic orientation, the optical azimuthal scans are carried out for the samples quenched at various periods of crystallization time during the same heat treatment process as for the birefringence measurement. Fig. 3 indicates that the samples quenched at 10 and 20 min exhibit the orientation because the intensity change obeys the equation, $I^2 \sim A\sin^2(2\phi)$, where ϕ is the azimuthal angle with respect to the magnetic field. The amplitude A is equal to $\sin^2(\pi d\Delta n/\lambda)$, which is the quantity observed in Fig. 2. In Fig. 3, the amplitude is larger for the sample quenched at 10 min than that quenched at 20 min,

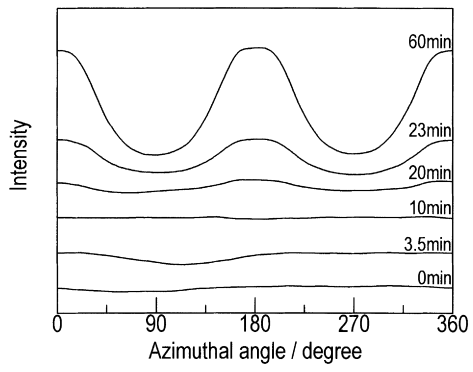

Fig. 5. X-ray azimuthal scans along (100) plane of the samples melted at 270°C and crystallized at 250°C, followed by quenching at various periods of crystallization time indicated in the figure. The zero azimuthal angle corresponds to the equatorial direction when the direction of the magnetic field is meridional.

but it is opposite in Fig. 2. This discrepancy could be attributed to the difference in sample thickness between the sample used in the in situ measurement (Fig. 2) and the sample prepared by quenching (Fig. 3). Even with the same temporal change in Δn, the oscillating rate depends on the sample thickness d. The samples quenched at 23 and 60 min do not clearly exhibit the azimuthal angle dependence, but this does not mean that there is no orientation. At a later stage of crystallization, the angular dependence becomes unclear because of the multiple scattering due to the crystallites formed. The scattering is enhanced because the sample is thick (200 μm) in comparison to the sample thickness for the in situ measurements.

Fig. 4 shows the X-ray equatorial diffraction profiles obtained for the same quenched samples as those used in the optical measurements. No crystallites are formed until the crystallization time up to 20 min. This crystallization time is well after the onset time of the increase in the transmitting light intensity shown in the birefringence measurement (Fig. 2). If we define the induction period of crystallization as the period in which no crystal formation is detected by means of WAXD, we could say that the magnetic orientation starts to occur during the induction period. The orientation, therefore, is not due to the crystals (detected by WAXD) but some anisotropic structure formed prior to the crystallization. However, the possibility of crystallite orientation is not ruled out because the WAXD is not sensitive to detect small amounts of disordered crystal. In addition, the origin of the anisotropic structure is not yet fully understood. One possibility of the origin is that the anisotropic structure is formed from purely isotropic melt in the course of crystallization. Another possibility is that some residual order remains due to the 'memory effect' even though the sample is heated above the melting point. Further investigation is under way regarding this point.

The orientation of the crystallites at the later stage of crystallization is observed by means of X-ray azimuthal scans. Fig. 5 shows the azimuthal scans along the (100) plane for the samples quenched at various crystallization times. The samples quenched before 20 min exhibit almost flat profiles. This is because no crystallites are formed yet at this time period. The samples obtained for 23 and 60 min, which exhibit crystallinity as seen in Fig. 4, clearly show the azimuthal profile characteristic of orientation.

In Fig. 6(a), the azimuthal scans along the different planes obtained for the sample heat-treated outside the magnet are shown. It is evident that no orientation is observed. In Fig. 6(b), the azimuthal scans along the different planes obtained for the sample heat-treated in the magnet are shown. The profile for the (010) plane indicates that the b^*-axis is aligned parallel to the magnetic field. The profile for the (100) plane indicates that a^*-axis is aligned roughly perpendicular to the magnetic field though the broad peak indicates that the actual direction of a^*-axis is inclined from the perpendicular direction to some extent. These observations on the directions of a^*- and b^*-axes with respect to the

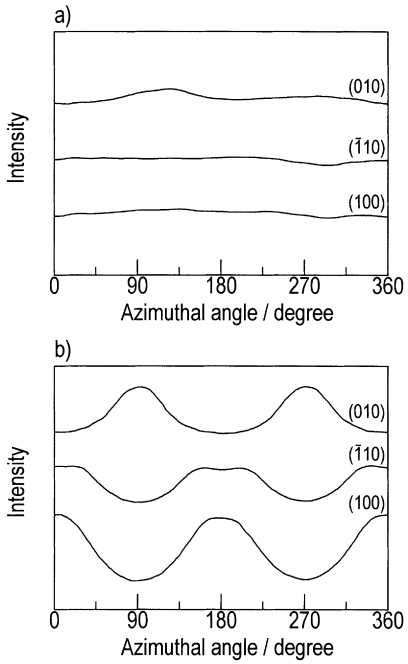

Fig. 6. X-ray azimuthal scans of the samples crystallized at 250°C for 60 min after melting at 270°C. Sample preparation was carried out (a) outside and (b) inside the magnet (6 T). The zero azimuthal angle corresponds to the equatorial direction when the direction of the magnetic field is meridional.

magnetic field are consistent with the triclinic crystal form of PET [14]. Although the azimuthal scans from the edge and end views were not carried out, a^*-axis is expected to be distributed symmetrically around the b^*-axis because of the axial symmetry of the magnetic field.

The perpendicular (though roughly) orientation of a^*-axis with respect to the magnetic field could be explained by the crystal structure of PET [14]. In the crystal of PET, the direction of a^*-axis lies approximately perpendicular to the plane of the aromatic ring. In the direction of the a^*-axis, the diamagnetic susceptibility $|\chi|$ is expected to be the largest due to a ring current induced on an aromatic ring in an external magnetic field. As a result, a^*-axis aligns perpendicular to the magnetic field so that the magnetic energy is minimized. It should be noted [15] that a^*-axis (or the a-axis) may not coincide with one of the three principal axes of the susceptibility because the crystal type of PET is triclinic. The ring current on an aromatic ring might be the main factor determining the orientation direction, but the following factors should also be considered. First, the contribution of the anisotropic diamagnetic susceptibility of the other chemical moieties in the repeating unit of PET, including the alkyl part [16–18] and carbonyl group, could not be ignored. Only a limited knowledge of χ of PET is available [19]. Second, the magnetic anisotropy of a repeating unit in a single chain is not necessarily the same as that in the crystal. Finally, conformations in the ordered domain, which is responsible for the magnetic orientation may be different from that in the crystal. In this case, the estimation of the susceptibility should be made not on the basis of the crystal but on the basis of the ordered structure.

The orientation of a^*-axis is reasonable in view of the above discussion. In contrast, the parallel orientation of the b^*-axis with respect to the magnetic field is not clearly explained in a straightforward manner. For better understanding, we need full information about three principal χ values of PET crystal. In addition, the knowledge of χ values of the ordered domain is important since the orientation starts to occur in the induction period, which might determine the final orientation of the crystals.

Acknowledgements

The authors express their thanks to Asahi Chemical for supplying PET samples.

References

[1] Belyi VA, Snezhkov VV, Bezrukov SV, Voronezhtsev YuI, Pinchuk LS. Dokl Akad Nauk SSSR 1988;302:355.
[2] Kimura T, Ezure H, Sata H, Kimura F, Tanaka S, Ito E. Mol Cryst Liq Cryst 1998;318:141.
[3] Sata H, Kimura T, Ogawa S, Ito E. Polymer 1998;39:6325.
[4] Ezure H, Kimura T, Ito E. Macromolecules 1997;30:3600.
[5] Sata H, Kimura T, Ogawa S, Yamato M, Ito E. Polymer 1996;37:1879.
[6] Kimura F, Kimura T, Sugisaki A, Komatsu M, Sata H, Ito E. J Polym Sci, Polym Phys Ed 1997;35:2741.
[7] Kimura T, Ezure H, Tanaka S, Ito E. J Polym Sci, Polym Phys Ed 1997;36:1217.
[8] Brostow W. In: Mark JE, editor. Physical properties of polymers handbook, New York: American Institute of Physics, 1996 chap. 33.
[9] Wunderlich B, Moller M, Grebowicz J, Baur H. Adv Polym Sci 1988;87:1.
[10] Wunderlich B, Grebowicz J. Adv Polym Sci 1984;60–61:1.
[11] Imai M, Kaji K, Kanaya S, Sakai Y. Phys Rev B 1995;52:12 696.
[12] Sakamoto Y, Kimura T, Kawai T, Ito E. Polym Prep Jpn 1998;47:1004.
[13] Sakamoto Y, Kimura T, Kawai T, Ito E. Polym Prep Jpn 1998;47:3843.
[14] de Daubeny RP, Bunn CW, Brown CJ. Proc R Soc (Lond) A 1954;226:531.
[15] Weiss A, Witte H. Magnetochemie, Weinheim: Bergstr Verlag Chemie GmbH, 1973 chap.3, Japanese translation.
[16] Weir EM, Selwood PW. J Am Chem Soc 1951;73:3484.
[17] Phaovibul O, Loboda-Cackovic J, Hosemann R, Balta-Calleja FJ. J Polym Sci, Polym Phys Ed 1973;11:2273.
[18] Balta-Calleja FJ, Berling KD, Cackovic H, Hosemann R, Loboda-Cackovic J. J Macromol Sci, Phys B 1976;12:383.
[19] Selwood Jr PW, Parodi JA, Pace A. J Am Chem Soc 1950;72:1269.